Economic Optimization of Hybrid PV-Battery Systems Using Hourly Satellite Insolation and Daily Temperature Data: A Case Study

Jeremy Every*, Li Li*, and David G. Dorrell†
*Faculty of Engineering and IT, University of Technology Sydney, Ultimo 2007, Australia
†Discipline of Electrical, Electronic and Computer Engineering, University of KwaZulu-Natal, Durban 4041, South Africa
Email: jeremy.every@student.uts.edu.au

***Abstract*—This paper presents an economic optimization case study for a medium-scale hybrid PV-battery system. PV energy yield and battery operation models based on hourly satellite insolation and daily temperature data form the basis of an underlying objective function aiming to maximize the net present value of potential energy cost savings. Forecasted system prices and energy tariffs over a nine-year period are considered enabling the opportune year to invest and the characteristics of the corresponding optimal system to be determined.**

***Index Terms*—Economic analysis, Energy storage, Particle swarm optimization, Photovoltaic systems**

I. Introduction

Despite significant cost reductions in recent years, hybrid PV-battery solutions are still burdened by the significant capital outlay required and rapidly changing regulatory conditions and incentive schemes. Consequently the optimization of system characteristics including power and energy ratings is necessary to establish the most economically efficient system for a particular application.

The economic performance of a hybrid PV-battery system is primarily dependent on the prevailing environmental conditions under which the proposed system is intended to operate and the underlying load which it is intended to supply. In an Australian context, PV systems contribute to the Australian Government's Renewable Energy Target (RET) and are therefore eligible for certain incentives depending on the size of the system installed. For systems of 100 kW or less, PV systems are deemed to be part of the Small-scale Renewable Energy Scheme (SRES) and receive incentives in the form of upfront Small-scale Technology Certificates (STC) [1] and may be eligible to receive feed-in tariffs from an energy retailer. However from 2017 to 2030, STCs are scheduled to be phased out complicating the investment decision process.

For PV systems larger than 100 kW, incentives are provided through Large-scale Generation Certificates (LGC) [1]. PV system developers and owners enter into a negotiated Power Purchase Agreement (PPA), most commonly with energy retailers. Under a PPA, the price to purchase LGCs from the PV installation is typically built into the total price paid for grid-exported energy. In the analysis presented later in this paper, PPA prices from \$60/MWh to \$140/MWh are considered to determine the effect on the economic viability of hybrid PV-battery systems.

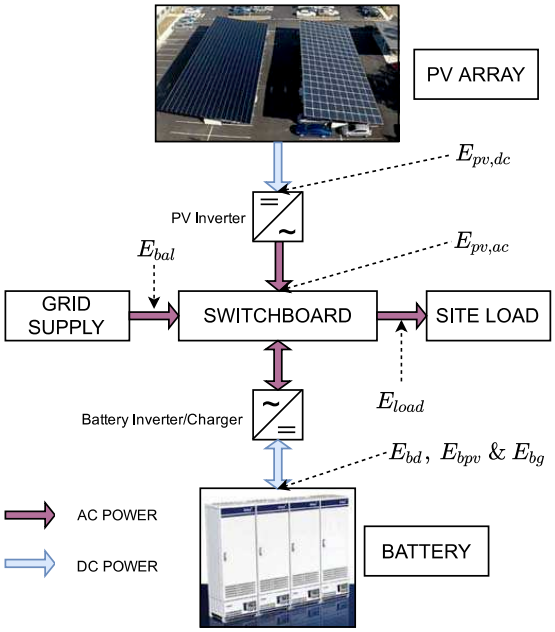

Fig. 1. TransGrid iDemand AC system.

A case study based on TransGrids iDemand project, featuring a 53 kW polycrystalline PV array combined with a 400 kWh lithium polymer battery system [2], is presented in the proposed paper. Operational data from the iDemand system is first used to validate the accuracy of the adopted PV energy yield model and then applied to hypothetical installations over a nine-year period to enable the determination of the opportune investment year and the characteristics and performance of the corresponding optimized system, including whether to install a small-scale or large-scale system given the different incentive schemes on offer. A block diagram of the TransGrid iDemand AC system is shown in Fig. 2. For a description of the energy flow terms refer to Section II.

This research is supported by an Australian Government Research Training Program Scholarship

In this paper, PV energy yield and battery lifetime operation models based on hourly satellite insolation and daily temperature data are considered. The objective function of the underlying optimization problem is formulated as a net present value (NPV) maximization of energy cost savings achieved through the introduction of an optimally sized and oriented PV-battery system. Consideration is given to forecasted technology cost reductions and electricity tariff increases.

II. Methodology

A. Hourly Insolation and Temperature Models

The Bureau of Meteorology (BOM) for the Australian Government maintains a database of hourly and daily insolation data from satellite observations. While direct access to the hourly data is available subject to a fee, the Australian Renewable Energy Agency (ARENA) has made hourly data from 1990 to 2015 available via the Australian Renewable Energy Mapping Infrastructure (AREMI) spatial data platform [3]. The data includes Global Horizontal Insolation (GHI) and Direct Normal Insolation (DNI) which are related through the following equation:

$$GHI = DNI \times \cos(\theta_z) + DHI \tag{1}$$

where DHI is the Diffuse Horizontal Insolation and θ_z is the solar zenith angle (an equation for which is established in [4]). Consequently through rearranging (1), DHI can be found from the AREMI data.

After obtaining the required insolation components based on satellite data, a transposition model is required to estimate the insolation on the plane-of-array (POA) of a PV system. Numerous transposition models have been developed however no universal model has been shown to be the most accurate. Consequently for the purposes of this research, the Hay-Davies-Klucher-Reindl (HDKR) model, defined in (2), is used.

$$\begin{aligned} I_T = {} & (I_b + A_i I_d)\, R_b \\ & + I_d(1 - A_i)\left(\frac{1+\cos\beta}{2}\right)\left[1 + f\sin^3\left(\frac{\beta}{2}\right)\right] \\ & + I\rho_g\left(\frac{1-\cos\beta}{2}\right) \end{aligned} \tag{2}$$

In (2), I_b and I_d are the hourly direct and diffuse insolation on the horizontal plane respectively, $A_i = I_b/I_o$, $f = \sqrt{I_b/I}$, I is the hourly global horizontal insolation, I_o is the hourly extraterrestrial insolation, ρ_g is the ground reflectance and R_b is the ratio of tilted to horizontal direct insolation. Importantly, R_b is a function of panel tilt β and panel azimuth γ, equations for which can be found in [4].

An Incident Angle Modifier (IAM), as defined by De Soto et al. [5], was also modelled to account for reflected radiation off the PV panel glass surface.

Hourly temperature data is typically unavailable for the vast majority of locations. Numerous empirical models have been developed to estimate hourly temperatures from daily minimum and maximum data. The hourly model defined by de Wit [6], constructed from piecewise sine functions has been shown to be one of the more accurate methods [7] and is therefore considered in the analysis presented in this paper. The model assumes the maximum and minimum daily temperatures ($T_{\max}$ and $T_{\min}$) occur at 2 pm and sunrise respectively [7]. The ambient temperature T_a at each hour based on the de Wit model is defined as follows:

$$T_a = \begin{cases} a + b\cos\left(\frac{\pi h'}{10+h_{rise}}\right) & \text{for } 0 \le h < h_{rise} \\ a + b\cos\left(\frac{\pi h'}{10+h_{rise}}\right) & \text{for } 14 < h < 24 \\ a - b\cos\left[\frac{\pi(h-h_{rise})}{14-h_{rise}}\right] & otherwise \end{cases} \tag{3}$$

where $a = (T_{\max} + T_{\min})/2$, $b = (T_{\max} - T_{\min})/2$, h is hour of the day, h_{rise} is the sunrise hour angle and $h' = h + 10$ if $h < h_{rise}$ and $h' = h - 14$ if $h > 14$. It should be noted that for $h > 14$, $T_{\min}$ of the next day is used to determine T_a for the remaining hours of each day.

The BOM Climate Data Online (CDO) database contains daily maximum and minimum temperature data for thousands of weather locations within Australia. Data for the station closest to TransGrid's iDemand site (less than 4.5 km away) is applied to (3) to estimate hourly ambient temperature.

B. PV Energy Yield Model

The PV energy yield model as defined in [4] is considered in this research. Efficieny factors similar to the ones considered by Copper et al. [8] are also applied.

The DC generated energy is defined as follow:

$$E_{pv,dc} = A_c Z I_T \eta_{mpp} \zeta_{pv} \eta_{soil} \eta_{mm} \eta_{dc,wire} \tag{4}$$

where A_c is the area of each PV module, Z is the number of PV modules, I_T is the insolation incident on the tilted plane, η_{mpp} is the module efficiency at the maximum power point and ζ_{pv} is the PV module degradation factor (according to the module datasheet). η_{soil}, η_{mm} and $\eta_{dc,wire}$ are the efficiencies due to panel soiling, module mismatch and DC wiring losses, assumed to be 99%, 98% and 98% respectively in this research. The PV module efficiency η_{mpp} is defined as follows:

$$\eta_{mpp} = \eta_{mpp,STC} + \mu_{mpp}(T_c - T_a) \tag{5}$$

where $\eta_{mpp,STC}$ is the efficiency at standard test conditions, μ_{mpp} is the the power temperature coefficient and T_c is the module operating temperature. T_a is the ambient temperature determined through (3). The equation for panel degradation factor has been previously defined in [9].

The total energy generated by the PV system as AC power is defined as:

$$E_{pv,ac} = E_{pv,dc} \eta_{inv} \eta_{ac,wire} \tag{6}$$

where $\eta_{ac,wire}$ is efficiency due to AC wiring losses assumed to be 99% and η_{inv} is the inverter losses. For this research, the inverter losses are assumed to be in accordance with the SMA STP17000TL model inverters installed in the iDemand system. The characteristics of the PV modules considered in this analysis are shown in Table III in the Appendix.

C. Battery Model

The battery model assumed in this research is based on the model previously developed by Every et al. [10], detail of which is excluded for brevity. The model assumes battery operation in line with the manufacturer's warranted performance. Furthermore, the battery operational characteristics are limited to the continuous operation ratings prescribed on the manufacturer's datasheets.

An energy storage system can also be used to perform energy arbitrage by charging during low cost off-peak hours and discharging during peak periods in addition to shifting PV generated energy to non-generation periods. In this paper, various battery operating modes are considered in the optimization algorithm to establish the most economically efficient operating profile. The operating modes considered are defined as follows:

- Mode 1: PV generation shifting. Discharge in peak only.
- Mode 2: PV generation shifting. Discharge during shoulder and peak periods.
- Mode 3: Energy arbitrage and PV generation shifting. Discharge in peak only.
- Mode 4: Energy arbitrage and PV generation shifting. Discharge during shoulder and peak periods.

The characteristics of the battery modules considered in this analysis are shown in Table IV in the Appendix.

D. Economic Assumptions

A nominal discount rate of 10% per annum is considered in this paper, representative of the cost of capital that may be expected for a large corporation such as TransGrid. Annual inflation is assumed to be 2.5% while nominal electricity price growth is taken to be 4.5%.

For larger scale commercial and industrial customers, electricity charges are typically billed monthly. Consequently the real discount rate and electricity price growth (taking inflation into account) converted to monthly effective rates are $r_d = 0.59\%$ and $r_e = 0.16\%$ respectively.

The analysis presented in this paper considers forecasted PV system, battery and battery inverter costs between 2017 and 2025. The forecasted costs are based on three price scenarios as defined by Brinsmead et al. [11], designated as minimum, base and maximum price scenarios.

E. Maintenance Model

System maintenance is an essential component of hybrid PV-battery system operation. While not explicitly defined in this paper, inverter, battery and PV array maintenance is assumed to occur once every five years at a cost of $300 for systems of size less than 1 MWh as previously assumed by Brinsmead et al. [11]. Inverter replacement is assumed to be required after 10 years while battery replacement is required when the end-of-life maximum capacity is reached or after 10 years, whichever occurs first. The replacement cost is assumed to be the forecasted price for the corresponding year in [11].

F. Optimization Problem

Find: Tilt angle β, azimuth angle γ, number of PV panels Z and number of batteries X

Objective:

$$\max_{\beta,\gamma,Z,X} NPV = \sum_{q=1}^{Q} \frac{(C_{base,q} - C_{pvbatt,q})(1+r_e)^q}{(1+r_d)^q} - \sum_{q=1}^{Q} \frac{W_q}{(1+r_d)^q} - \left(S_{pvbatt}\right) \tag{7}$$

Subject to:

$$0 \leq \beta \leq 180 \quad \text{for } \beta \in \mathbb{R} \tag{8a}$$
$$-180 < \gamma \leq 180 \quad \text{for } \gamma \in \mathbb{R} \tag{8b}$$
$$0 \leq Z \leq Z_{\max} \quad \text{for } Z \in \mathbb{Z}^+ \tag{8c}$$
$$0 \leq X \leq X_{\max} \quad \text{for } X \in \mathbb{Z}^+ \tag{8d}$$

In (7), $C_{pvbatt,q}$ and $C_{base,q}$ represent electricity costs in billing period q with and without a hybrid PV-battery system respectively, W_q is the maintenance/replacement cost in period q and S_{pvbatt} is initial hybrid PV-battery system installation cost.

The terms $C_{base,q}$ and $C_{pvbatt,q}$ are defined as:

$$C_{base,q} = \sum_{d=1}^{D} \left(\sum_{h=1}^{24} T_{E,qdh} E_{load,qdh} + T_{D,qd} \right) + T_{DC,q} P_{max,q} \tag{9}$$

$$C_{pvbatt,q} = \sum_{d=1}^{D} \left\{ \sum_{h=1}^{24} \Big[T_{E,qdh} \max(0, E_{bal,qdh}) - T_{pv,qdh} \max(0, -E_{bal,qdh}) \Big] + T_{D,qd} \right\} + T_{DC,q} P_{\max,q} \tag{10}$$

where $T_{E,qdh}$ is the cumulative energy charge in Table V (expressed in c/kWh) for the h^{th} hour of day d with D days in the billing period, $T_{D,qd}$ is the cumulative daily supply charge, $T_{DC,q}$ is the demand charge for the billing period, $P_{\max,q}$ is the maximum demand within the billing period and $T_{pv,qdh}$ is the tariff paid to the system owner for surplus energy generated. For systems of size $\leq$100 kW, $T_{pv,qdh}$ is the retailer PV feed-in tariff (6c/kWh) and for large-scale systems ($>$100 kW) $T_{pv,qdh}$ is the supply rate as agreed in the PPA (ranging from $60/MWh to $140/MWh). $E_{bal,qdh}$ is the net energy flow balance expressed as:

$$E_{bal,qdh} = E_{load,qdh} - E_{pv,qdh} - E_{bd,qdh} + E_{bpv,qdh} + E_{bg,qdh} + E_{bloss,qdh} \tag{11}$$

where $E_{load,qdh}$ is the load energy, $E_{pv,qdh}$ is PV generated energy, $E_{bd,qdh}$ is the energy discharge from the battery, $E_{bpv,qdh}$ and $E_{bg,qdh}$ are the charge energies from the pv system and grid respectively and $E_{bloss,qdh}$ is the energy

lost during charge/discharge. For a complete definition of the battery energy flow terms, refer to [10].

The energy costs associated with the terms $T_{E,qdh}$, $T_{D,qd}$ and $T_{DC,q}$ are shown in Table V in the Appendix.

As the problem is in the form of a mixed integer non-linear programming problem, meta-heuristic methods were employed to solve the problem. A modified version of particle swarm optimization, known as comprehensive learning quantum-behaved particle swarm optimization (CLQPSO) was employed. QPSO has been shown have a better global search performance that standard PSO with fewer parameter adjustments [12]. The CL component as proposed by [13] and applied to QPSO by [14] further improves the global search performance. The optimization problem was solved using Matlab 2017a.

III. Results

A. Energy Model Comparison

A comparison of average hourly generated AC power from the 53 kW polycrystalline silicon PV array installed by TransGrid and the energy production model considered in this research is presented in Fig. 2. Plots for energy production for months centred around winter and summer, as well as a full year of production are shown. For the full year of production, the energy model appears to slightly underestimate energy production in the late morning and afternoon hours and overestimates production in the early morning. The overall normalized mean bias error (NMBE) for the full year of AC production was found to be 0.02% as shown in Table I.

The overestimation during early morning can be attributed to shading events in winter, clearly observed in the winter plots of Fig. 2. The model inaccuracy due to shading events is further demonstrated by the NMBE and normalized root mean square error (NRMSE) statistics summarized in Table I which are the worst for the three periods assessed. The overall accuracy of the PV energy yield model is perhaps better represented by the statistics for the summer period whereby the NRMSE is the lowest amongst periods assessed and the overall NMBE for AC energy is -2.9%.

The overall effect of energy yield model inaccuracy on the determination of economic performance of a PV system is shown in Table II. The model underestimates electricity cost savings by just 1.57%, thereby presenting a conservative estimate. Based on the relatively low error, a reasonable degree of confidence in accuracy of the PV energy yield model can be held for the purposes of economic optimization.

The average hourly load profiles in different seasons are also shown in Fig. 2. Clearly there is a strong alignment between the hours of electricity demand and the hours of energy generation. The significance of this load profile is further discussed in Section IV.

B. Optimization Results

Following the application of the optimization algorithm applied to the TransGrid iDemand data and the economic scenarios considered, no hybrid PV-battery system was found to yield an economic benefit greater than a PV-only system. Consequently, the results presented and discussed in the remainder of this paper refer to a PV-only system.

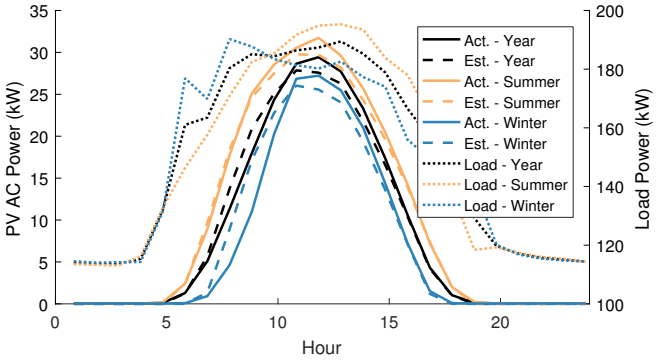

Fig. 2. Comparison of average hourly estimated AC generation versus actual measured AC generation in 2015.

TABLE I
NORMALISED STATISTICS FOR MEASURED VERSUS MODELLED ENERGY PRODUCTION OF IDEMAND SYSTEM

Period	AC Energy		DC Energy	
	NMBE (%)	NRMSE (%)	NMBE (%)	NRMSE (%)
Year	-0.02	24.18	-0.36	24.19
Summer	-2.9	20.69	-3.24	20.81
Winter	4.36	29.34	4.01	29.22

Referring to Fig. 3, the NPV achieved for an optimized system steadily increases with installation year due to reduction in system costs. For the base pricing scenario shown in Fig. 3, it can be seen that the optimal system size for the load profile considered is a 100 kW PV system, the maximum achievable under the small-scale renewable energy scheme, up until 2022. Between 2023 and 2025, the optimal system from an NPV perspective would be a large-scale system. At this point, the NPV and system size trajectories diverge depending on the negotiated exported energy price under a PPA. It should be noted that the distinct NPV increase from 2021 to 2022 is due to a significant price drop as forecasted by Brinsmead et al. [11] and is unrelated to the pricing scenario and PPA energy price.

Referring to Fig. 4, the modified internal rate of return (MIRR) for an investment in PV steadily increases as system price are expected to decrease overtime. Due to the forecasted price drop in 2022, the MIRR increases rapidly before reducing once again as the optimal system is deemed to be a large-scale scale system. The inverse is true for the payback period.

TABLE II
NPV OF ENERGY COST SAVINGS OF IDEMAND SYSTEM (2015)

NPV (Actual)	NPV (Estimated)	Error (%)
$10,210	$10,049	-1.57

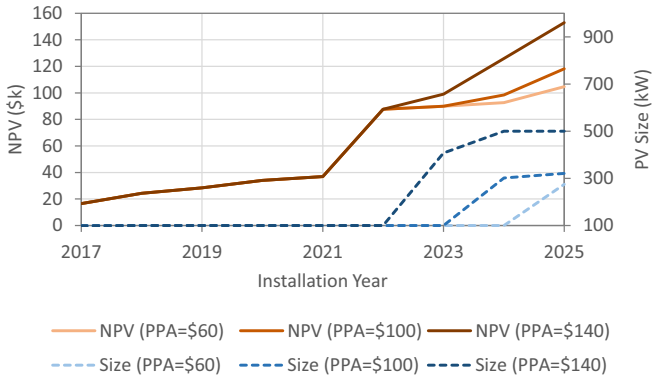

Fig. 3. Optimal PV array sizes and associated NPVs evaluated for a range of PPAs forecasted for future years of installation.

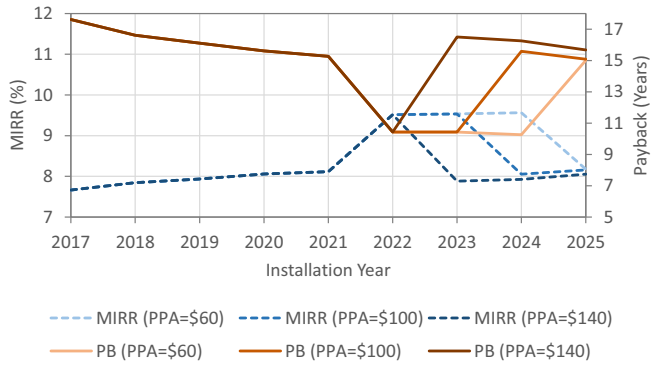

Fig. 4. MIRR and payback periods of optimized systems for a range PPAs forecasted for future years of installation.

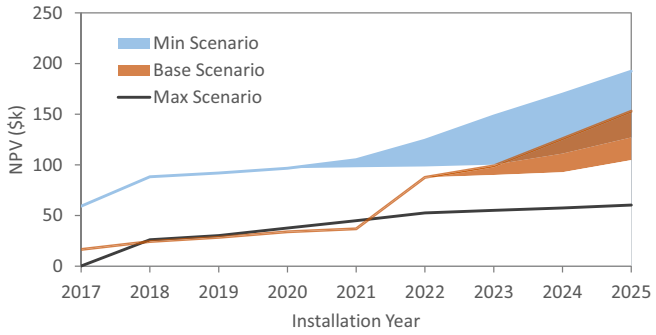

Fig. 5. Comparison of optimized NPVs for three component pricing scenarios (min, base and max). Overlaid shaded areas represent the range of PPAs considered (lower bound represents $60/MWh, upper bound represent $140/MWh).

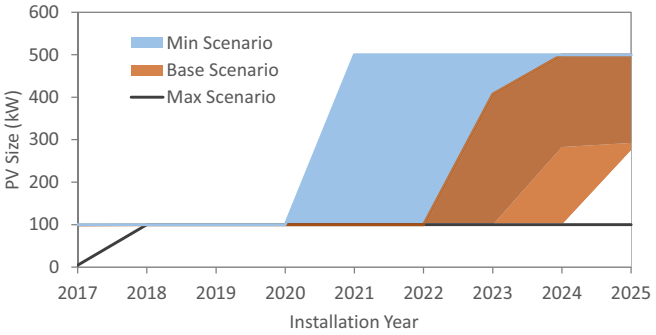

Fig. 6. Comparison of optimal system sizes for three component pricing scenarios (min, base and max). Overlaid shaded areas represent the range of PPAs considered (lower bound represents $60/MWh, upper bound represent $140/MWh).

It should be noted that under the base system pricing scenario featured in Figs. 3 and 4, the maximum MIRR achieved for the NPV optimized PV systems is around 9.5%, less than the cost of capital of 10%. Consequently, without considering ulterior motives, under the economic assumptions considered in this paper, investment in a PV system does not present the most efficient investment option. However a relaxation of the discount rate, would yield a higher rate of return and therefore the investment in a PV system may be deemed economically viable.

The optimal NPV and PV system size trajectories for the three pricing scenarios considered in this research are overlaid in Figs. 5 and 6 respectively. Under the minimum and base price scenarios, the optimal system size is 100 kW until 2020 and 2022 respectively whereby a larger system is the most beneficial. The shaded regions represent the range of PPA energy prices considered in this research, the lower bound representing $60/MWh and the upper bound representing $140/MWh. However under the maximum price scenario, the optimal size for all installation years is almost uniform at 100 kW with the exception of the initial year 2017. Due to especially high PV system costs modelled for 2017 under the maximum pricing scenario, the optimal size is only 4.5 kW. This is an unrealistic scenario as the industry pricing is currently tracking well below the assumed price point.

IV. Discussion

It should be noted that hourly insolation measurements from satellite observations do not necessarily coincide with the beginning of the hour. In the instance of MTSAT-2 observations at a latitude of -35°, the observation occurs 49.5 seconds after the beginning of the hour [15]. As the insolation observations are required to align with the time stamp for the load data, this may present a problem. Consequently hourly insolation estimates based on daily insolation data may be required where load data is not available in minutely intervals, such as has been previously investigated in [9].

As stated in Section III, no battery system was found to provide an economic benefit higher than a PV-only system. This may be attributed to two primary factors. Firstly, the electricity costs as detailed in Table V are particularly low when compared to the residential consumer market. Consequently, the relatively low energy cost savings achieved through avoided grid-imported energy are not sufficient to outweigh the high capital costs of a battery system. Secondly, as shown in Fig. 2, the hours of load demand strongly align with the hours of PV generation. Therefore, the benefit achieved through shifting PV generated energy to peak hours

is far less than the case if demand occurs during the peak tariff period. The combination of these two factors mean that under the load profile and tariffs conditions representative of TransGrid's operations, a hybrid PV-battery system is not the most economically efficient arrangement.

V. Conclusion

PV energy yield models and battery operation models were developed as key components of an optimization algorithm to determine the hybrid PV-battery system with the most economic value for a load based on TransGrid's iDemand system. The energy yield model was found to have an acceptable accuracy and shown to underestimate the potential annual energy cost savings by just 1.57%.

Implementation of the optimization algorithm revealed no battery system would yield an economic benefit greater than a PV-only system for installation years between 2017 and 2025. Under the system pricing scenarios considered, the optimal system was found to be a small-scale system until 2020 after which a transition to a large-scale system would yield the highest net present value depending on the pricing scenario considered.

The results presented in this article demonstrate the necessity to optimize PV-battery systems as an integral component of the investment decision process.

Appendix

TABLE III
PV module characteristics

Make	Suntech
Model	STP250-20/Wd
Type	Polycrystalline
Maximum Power @ STC	250 W
Efficiency ($\eta_{mpp,STC}$) @ STC	15.4% W
Power temperature coefficient (μ_{mpp})	-0.43%/°C
NOCT	45°C
Surface Area (A_c)	1.62688 m

TABLE IV
Battery characteristics

Manufacturer	Kokam
Model	KRI-H-3R4C-133
Nominal Charge/Discharge Power (R_{max})	133 kWh
Initial Maximum Useful Capacity ($C_{\max 0}$)	126 kWh
End-of-life Capacity (C_{EOL})	75.6 kWh (60%)
Cycles (Y_{EOL})	8000
Depth of Discharge (D)	80%
Round-trip DC efficiency (η_{batt})	95%
Assumed warranty period	10 years

TABLE V
Electricity charges (P=Peak, SH=Shoulder, OP=Off-peak)

Charges	Rate			Unit
	P	SH	OP	
Retailer Energy	6	6	4	c/kWh
Distributor Energy	4.1124	3.0474	1.3178	c/kWh
Distributor Demand	10.4581			$/kVA
Network Access Charge	18.729			$/Meter/Day
Administration	0.0378			c/kWh
Ancillary Services	0.261			c/kWh
Meter Provision	2			$/Meter/Day
LRET	0.381			c/kWh
SRES	0.404			c/kWh
NSW Energy Saving	0.082			c/kWh

References

[1] (2015, 2 June) Financial incentives. Australian Government Clean Energy Regulator. [Online]. Available: http://www.cleanenergyregulator.gov.au/RET/How-to-participate-in-the-Renewable-Energy-Target/Financial-incentives

[2] "iDemand: A technical guide to TransGrid's Western Sydney electricity demand management system," TransGrid, Sydney, 2015 2015.

[3] (2017, 30 May) Australian renewable energy mapping infrastructure. Australian Renewable Energy Agency. [Online]. Available: https://nationalmap.gov.au/renewables/

[4] J. A. Duffie and W. A. Beckman, *Solar engineering of thermal processes*. Hoboken, N.J.: Wiley, 2013, vol. 4th.

[5] W. De Soto, S. A. Klein, and W. A. Beckman, "Improvement and validation of a model for photovoltaic array performance," *Solar Energy*, vol. 80, no. 1, pp. 78–88, 2006.

[6] C. T. de Wit, *Simulation of assimilation, respiration, and transpiration of crops*. Wageningen: Pudoc, 1978.

[7] D. Reicosky, L. Winkelman, J. Baker, and D. Baker, "Accuracy of hourly air temperatures calculated from daily minima and maxima," *Agricultural and Forest Meteorology*, vol. 46, no. 3, pp. 193–209, 1989.

[8] J. K. Copper, A. B. Sproul, and S. Jarnason, "Photovoltaic (PV) performance modelling in the absence of onsite measured plane of array irradiance (POA) and module temperature," *Renewable Energy*, vol. 86, pp. 760–769, 2016.

[9] J. Every, L. Li, and D. G. Dorrell, "Leveraging smart meter data for economic optimization of residential photovoltaics under existing tariff structures and incentive schemes," *Applied Energy*, vol. 201, pp. 158–173, 2017.

[10] ——, "Optimal selection of small-scale hybrid PV-battery systems to maximize economic benefit based on temporal load data," 2017, unpublished (presented at 12th International Conference on Industrial Electronics and Applications, Siem Reap, Cambodia). [Online]. Available: https://arxiv.org/abs/1705.10949

[11] T. Brinsmead, P. Graham, J. Hayward, E. Ratnam, and L. Reedman, "Future energy storage trends: An assessment of the economic viability, potential uptake and impacts of electrical energy storage on the NEM 2015-2035," CSIRO, Report EP155039, September 2015.

[12] J. Sun, C.-H. Lai, and X.-J. Wu, *Particle swarm optimisation*. Boca Raton, Fla.: CRC Press, 2012.

[13] J. J. Liang, A. K. Qin, P. N. Suganthan, and S. Baskar, "Comprehensive learning particle swarm optimizer for global optimization of multimodal functions," *IEEE Transactions on Evolutionary Computation*, vol. 10, no. 3, pp. 281–295, 2006.

[14] H. Long and X. Zhang, *Quantum-Behaved Particle Swarm Optimization Based on Comprehensive Learning*. Berlin, Heidelberg: Springer-Verlag, 2012, pp. 15–20.

[15] "Gridded hourly solar global horizontal irradiance metadata," Australian Government Bureau of Meteorology, 15 November 2016. [Online]. Available: http://www.bom.gov.au/climate/data-services/docs/Metadata_IDCJAD0026_gridded_hourly_GHI.pdf